


Cite this: *RSC Adv.*, 2017, 7, 35368

Starch-based and multi-purpose nanofibrous membrane for high efficiency nanofiltration†

Sarekha Woranuch, Autchara Pagon, Kantapat Puagsuntia, Nakarin Subjaleearndee and Varol Intasanta *

The objective of the present work is to develop nanofibrous membranes from rice-flour based nanofibers containing PVA for high efficiency filtration. Rice flour-based biodegradable nanofibrous membranes were prepared by an electrospinning technique. The contents of the rice flour in solution were systematically varied before 25% w/w was set as an optimal condition where good processability, fibers with well-defined morphology and uniform diameter could be successfully achieved for both polymer and polymer nanocomposite. The rice flour nanofibrous membranes allow only tiny particles to pass through (less than 0.1 micron). Likewise, the incorporation of silver nanoparticles and β -cyclodextrin into the nanofibrous membranes leads to improved antimicrobial properties and volatile organic compound adsorption, respectively. The results suggest the potential use of nanofibrous membranes from rice flour blends as low-environmental impact and high performance multipurpose nanofilters.

Received 7th July 2017
Accepted 10th July 2017

DOI: 10.1039/c7ra07484k

rsc.li/rsc-advances

1. Introduction

High efficiency and multipurpose filters are of scientific, technological and social impact.^{1,2} As the need for clean air manifests into business demand for effective air treatment systems and products,³ nanofiltration has emerged as a promising route toward elimination of ultrafine particles. Yet, particulate barrier is only one among other crucial aspects of filtration. Bacterial elimination and toxic gas prevention could also account for the expected efficiency of advanced filtration.^{4,5} In addition, ultra-high efficiency filtration requires frequent replacement as dust could quickly accumulate and increase the pressure drop. As such, disposable filters are highly preferred when the active parts are made of ultrafine porous membrane.

In recent years, active components for filtration have stemmed from membranes,⁶ filter papers⁷ and microfibers.⁸ However, each type of component was inherited with different kind of drawbacks. Flexible and cost-effective, filter papers have low filtration efficiency as their inner structures were made of micron-sized cellulose short and long fibres.⁹ Despite their natural bending strength, filters made of synthetic microfibers also suffered low filtration efficiency due mainly to their micron-sized internal porous structures.⁸ Costly, several porous membranes lack required flexural strength for the final products to be pleated into various kinds of filters.¹⁰

As efforts have been made to overcome such multiple weaknesses associated with existing filter systems, nanofibrous membranes have emerged as one of the most promising alternative to high efficiency filtration.¹¹ Their fibrous nature has made these key components not highly effective but also structurally flexible. Formed by deposited nanofibers on a substrate, nanofibrous membranes could be made into thin, light and highly flexible within apparently flat arrangement with micro-to-nano sized internal structures depending of the sizes of the constituting fibers. Several nanofibrous membranes have been fabricated from solutions by hydrothermal,¹² electrospinning¹³ and forced spinning.¹⁴ Among these approaches, electrospinning has been popularized and vastly explored for both scientific investigations and industrial productions.¹³

Having a potential for fabrication of stand-alone nanofibrous membranes, electrospinning could be employed to produce long and continuous fibrous structures, the features highly associated with both tensile and flexural strength.¹⁵ The resulted functional nanofibers could be derived from both embedded functional components added into the precursor solution prior to spinning^{16,17} and post-spinning surface modifications by treating the membrane with desirable functional chemicals.^{17,18} While the latter has proved convenient, the first approach was considered more effective because the implantation of materials could translate into permanent functions over subsequent usages and applications.^{19,20}

Nevertheless, the uses of nanofibrous membrane in filtration might encounter challenges associated with both high pressure drop and short runtime due to accumulated particles blocking aerial pathways.^{17,21} Even though engineering design could be introduced to palliate such problems, it has been well-accepted

Nano Functional Textile Laboratory, National Nanotechnology Center (NANOTEC), National Science and Technology Development Agency (NSTDA), 111 Thailand Science Park, Pathumthani, 12120, Thailand. E-mail: varol@nanotec.or.th; Fax: +66 2 564 6981; Tel: +66 2 564 7100 ext. 6580

† Electronic supplementary information (ESI) available. See DOI: 10.1039/c7ra07484k



that maintenance and replacement were imminent for any types of filters.²² Such disposal could finally lead to accumulating waste and need for attritions.²³ It could be deduced from the above rationale that, while nanofibrous membranes could have potential in high efficiency filtration and engineering set up could help improve the throughput, their clearance remained environmentally problematic and needed research and development attention.

We were interested in developing multifunctional nanofibrous filters with the main component made of degradable materials derived from renewable resources. In addition to biodegradability, antibacterial function and VOC absorbing property were to be incorporated in our investigation.^{24–27} The two auxiliary features were to play a beneficial part in such advanced high efficiency filtration as for medical operation and microelectronic clean rooms.¹⁷ As such, rice starch became one of the most promising target materials which could offer both structural integrity and disposability with low environmental impact due to its cellulosic features.²⁴

Derived from rice flour, rice starch could be processed alkaline steeping method.²⁸ This class of cellulosic materials was a well-recognized polysaccharides with a rich variety of amylose–amylopectin combinations.²⁹ As a main component, amylose composed of a linear chain and constituted to the amorphous part of starch granule. In contrast, amylopectin represented branched molecules and contributed to the crystalline component. The interactions and variation between these two key components led to vast variety of rice with different physical structure and mechanical properties.^{30,31} For their unparalleled combinatorial characteristics including non-toxicity, biodegradability, biocompatibility, and ability to form films, membranes, gels, and fibers, starches have been of both scientific and industrial interest.^{32–34}

Recently, we studied the fabrication of rice starch-based functional nanofibers by investigating the relevant solution parameters.³⁵ Obtained by simple physical grinding without any further purification process, rice flour was chosen to fabricate bio-based nanofibers. PVA was introduced to facilitate both solution stability and fiber formation, as electrospinning of water-based rice flour solution has proven difficult. We found that the viscosity of precursor solutions, morphology, chemical structure, crystallinity, thermal characteristics of and mechanical property of resulted nanofibers were strongly influenced by rice flour content.

The objective of the present work was to develop nanofibrous membranes from rice flour for high efficiency filtration. Rice flour-based biodegradable nanofibrous membranes were prepared by electrospinning technique. The contents of rice flour in solution would be systematically varied before an optimal condition where good processability, fibers with well-defined morphology and uniform diameter could be successfully achieved for both polymer and polymer nanocomposite. Filtration efficiency would be evaluated as only tiny particles (less than 0.1 micron) were allowed to pass through. Subsequently, silver nanoparticles and β -cyclodextrin would be incorporated into the nanofibrous membranes for improved antimicrobial property and volatile organic compound

adsorption property. Finally, the potential use of such nanofibrous membranes from rice flour blends as low-environmental impact and high performance multipurpose nanofilter would finally be elaborated.

2. Materials and methods

2.1. Materials

Rice flour was supplied by Bureau of Rice Research and Development, Thailand. Polyvinyl alcohol (PVA, $M_w \sim 205\,000\text{ g mol}^{-1}$), silver nitrate (AgNO_3), β -cyclodextrin ($\text{C}_{42}\text{H}_{70}\text{O}_{35}$) and sodium hydroxide (NaOH) were obtained from Sigma-Aldrich, Germany. Deionized water was used in all experiments.

2.2. Preparation of electrospinning solutions

Ten electrospinning precursor solutions were prepared using different compositions, as shown in Table 1. PVA solution (8% w/w) was prepared by first dispersion of PVA pellets in distilled water followed by magnetic stirring for 2 h at 95 °C. In similar manner, rice flour solution (8% w/w) was prepared in 0.2 mM of sodium hydroxide with magnetic stirring for 24 h at 80 °C. The PVA solution, rice flour solution and other additional additives (AgNO_3 and β -cyclodextrin) were mixed at weight ratio of rice flour solution to PVA solution of 25 : 75 and then stirred for 24 h at room temperature.³⁵ Rice flour/PVA blend solution was named as NF whereas the ones with AgNO_3 at a concentration of 0.05 M, 0.1 M and 0.2 M were coded as NFS1, NFS2 and NFS3, respectively. NF solutions with β -cyclodextrin solid content for 10% w/w, 20% w/w and 40% w/w were coded as NFB1, NFB2 and NFB3, respectively. NF containing 0.2 M of AgNO_3 and 20% w/w of β -cyclodextrin was coded as NFSB. The viscosity values of these solutions were given in Table 1.

2.3. Preparation of the electrospun nanofibers

Electrospinning was carried out using Nanospider technology (Nanospider laboratory machine NS LAB 500S, Elmarco s.r.o.). A precursor solution (25 mL) was fed into the Nanospider's 50 mL semi cylindrical reservoir, equipped with wire electrodes connected to a high-voltage supply. During the process, the electrode was rotated at 8 rpm. The distance between the rotating wire electrode and the ground electrode was 18 cm. In this work, the applied voltage was set at 65 kV.

2.4. Morphological analyses of electrospun nanofibers

Morphological analyses were done using Scanning Electron Microscopy (SEM) Hitachi E-1010 (Hitachi High-Technologies Corp., Japan). A prospective sample was fixed on a specimen stub with carbon adhesive tape and sputter-coated with a thin layer of gold. Finally, SEM micrographs were collected at an accelerating voltage of 20 kV and working distance of 5 mm. Average diameters of fibers were analyzed using image analysis software (Image-J) and calculated by selecting 10 fibers randomly observed on the SEM images.



Table 1 Composition and average diameter of nanofibers

| Sample | Additives | | Viscosity of electrospun solution ^a (cP) |
|------------|---------------------------|-----------------------------------------|-----------------------------------------------------|
| | AgNO ₃ (molar) | β-Cyclodextrin (% w/w of solid content) | |
| Rice flour | — | — | 250 ± 26.35 |
| PVA | — | — | 239 ± 23.98 |
| NF | — | — | 339 ± 23.98 |
| NFS1 | 0.05 | — | 338 ± 21.32 |
| NFS2 | 0.1 | — | 345 ± 22.85 |
| NFS3 | 0.2 | — | 341 ± 20.11 |
| NFB1 | — | 10 | 337 ± 20.12 |
| NFB2 | — | 20 | 338 ± 17.23 |
| NFB3 | — | 40 | 340 ± 25.84 |
| NFSB | 0.1 | 20 | 339 ± 27.46 |

^a Viscosity of electrospun solutions was determined with a Brookfield viscometer (DV-III cone ultra programmable rheometer, Brookfield Engineering Laboratories, USA).

2.5. Crystallinity of nanofibers

X-ray diffraction (XRD) patterns were recorded by a Bruker D8 Advance X-ray diffractometer (Germany) over a 2θ range from 5° to 60° with a scan rate of $0.04^\circ \text{ min}^{-1}$. The degree of crystallinity (X_c) was calculated from eqn (1):

$$X_c (\%) = (A_c / [A_c + A_a]) \times 100 \quad (1)$$

where A_c represented the area under the peaks representing the total crystalline region and A_a represented the area under the peaks representing the total amorphous region.

2.6. Antimicrobial activity of nanofibers

Antibacterial activity of an electrospun nanofibrous sample was evaluated against AATCC-147-2014 method, with *Escherichia coli* and *Staphylococcus aureus* as model microbes. The sample was placed above an inoculated nutrient agar plate for close contact. The plate was then incubated at 37°C overnight and analyzed for zone of inhibition. The antibacterial degree could be evaluated from the size of inhibition zone.

2.7. Absorption of volatile organic compound (VOC)

The VOC-absorbing capability of the nanofibers was investigated by exposing them to toluene vapor. For this experiment, 10 mL of toluene was placed onto a glass Petri dish and transferred to the bottom of a desiccator (diameter 30 cm, height 30 cm). Then, 20 mg of nanofibers were placed into the desiccator. The nanofibers were kept in toluene vapor for 24 h. Then nanofibers were removed from desiccator and kept in a suction hood for 3 h to remove free toluene or only adsorbed on surface of the sample. The amount of entrapped toluene was examined by using Fourier Transform Infrared Spectroscopy (FTIR). FTIR spectra were obtained with a Nicolet 6700 (Thermo Scientific, Inc., United States) using 128 scans at a resolution of 2 cm^{-1} over a wavenumber range of $500\text{--}4000 \text{ cm}^{-1}$.

2.8. Tensile testing of nanofibers

Mechanical properties of the samples were examined by the ASTM D882 method, using an Instron Model 5566 testing machine (UK). A nanofibrous sample was cut into a rectangular shape ($5 \text{ cm} \times 1 \text{ cm}$) prior to testing. The test was performed using a load cell of 1 kN, a crosshead speed of 10 mm min^{-1} and a grip separation of 10 mm. Ten replicates were tested for each sample to obtain an average value. The film thickness was measured at five positions on the perimeter and at the center of the film by a digital caliper to obtain an average value.

2.9. Air permeability of nanofiber on filter paper

Air permeability was determined by the ASTM D 737 method using an air permeability tester (model M021A; SDL Atlas, USA) with a testing head of 20 cm^2 . The air permeability test was performed at constant air pressure of 100 pascal. The results acquired from the tester were taken in units of $\text{cm}^3 \text{ s}^{-1} \text{ cm}^{-2}$. Five replicates were tested for each sample.

3. Results and discussion

3.1. Morphology of nanofibers

In Fig. 1a, it could be seen that electrospinning of pure rice flour solution resulted in no fibers as unveiled by SEM. In stark contrast, PVA solution led to smooth and dimensionally uniform nanofibers with the mean diameter of $158 \pm 23 \text{ nm}$ (Fig. 1b). The blend nanofibers with rice flour weight content of 25% w/w (NF) also exhibited physical uniformity with the average diameter of $151 \pm 36 \text{ nm}$ (Fig. 1c). The result indicated that PVA provided good spinnability which was consistent with a previous investigation on PVA/starch blends reported by Liu and He (2014).³⁶ Five precursor formulations containing a small amount of particulate nanosilver and β -cyclodextrin (NFS1, NFS2, NFB1, NFB2 and NFB3) gave rise to continuous nanofibers with the mean diameter in the range of $150 \pm 27\text{--}153 \pm 28 \text{ nm}$ (Fig. 1d, e, g, h and j, respectively). However, increased amount of silver (at 0.2 molar) or β -cyclodextrin (at 30% w/w of solid content) resulted pronounced appearance of beaded nanofibers with an average diameter of $150 \pm 11 \text{ nm}$ and $149 \pm 21 \text{ nm}$, respectively (Fig. 1f and i). This might be due to perturbed polymer chain entanglement at relatively high content of nanosilver.

3.2. Crystallinity

The crystallinity of nanofibers was analyzed by XRD technique. Rice flour exhibited diffraction peaks at 2θ of 15.2° , 17.6° , 18.3° and 23.1° , corresponding to A-type crystal structure (Fig. 2a).^{37,38} PVA nanofibers showed a major peak at 19.8° (Fig. 2b).³⁹ Fig. 2c displayed XRD patterns of silver nanoparticles at 38.3° and 44.5° (ref. 40) and of β -cyclodextrin at 12.7° and 19.7° (Fig. 2d).⁴¹ NF nanofibers exhibited a distinctive diffraction peak at 19.8° attributed to crystalline domain of PVA (Fig. 2e). Meanwhile, incorporation of silver nanoparticles and β -cyclodextrin did not affect the crystal type of NF (Fig. 2f–h). However, the peak at 38.3° became prominent in NF containing silver nanoparticles (Fig. 4f and h).



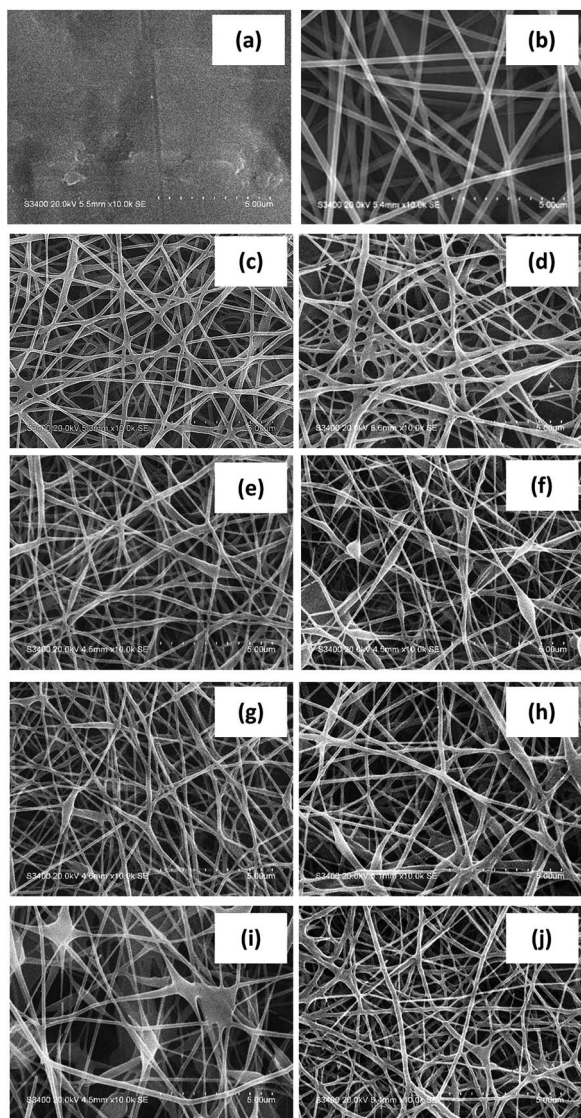


Fig. 1 SEM micrographs at 20 kV of different nanofibers: (a) rice flour, (b) PVA, (c) NF, (d) NFS1, (e) NFS2, (f) NFS3, (g) NFB1, (h) NFB2, (i) NFB3 and (j) NFSB.

The degree of crystallinity of PVA was calculated by eqn (1) to be 35.16%. Compared with PVA nanofibers, NF showed higher crystallinity of 37.82% (Table 2). At the same time, crystallinity of NF nanofibers increased by adding silver nanoparticles and β -cyclodextrin (53–60%). It was hypothesized that the two additives function as nucleating agents which promoted further crystallization of PVA.

3.3. Antimicrobial activity

Silver nanoparticles have the ability to anchor to the bacterial cell wall and subsequently penetrate it, thereby causing structural changes on the cell membrane such as hole creation and subsequently death of the cell.⁴² In general, silver nitrate and reducing agent are used as starting materials for the preparation of silver nanoparticles. Different reducing agent such as glucose, sodium hydroxide, sodium borohydride and elemental

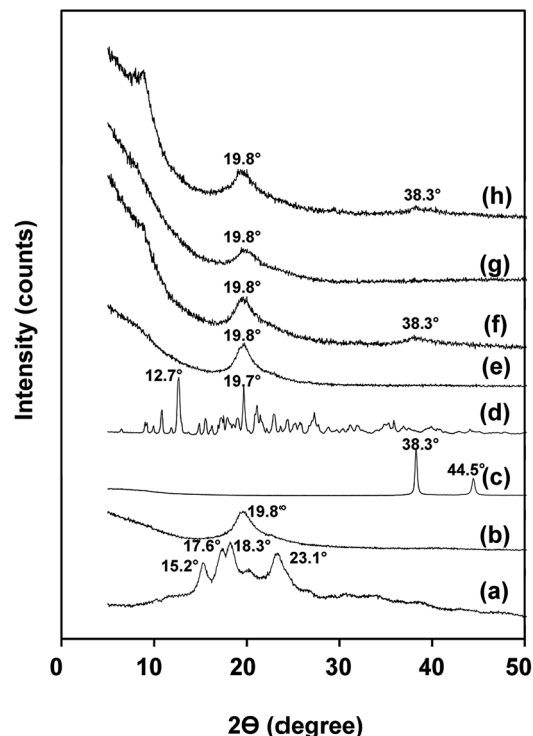


Fig. 2 X-ray diffractograms of: (a) rice flour, (b) PVA nanofibers, (c) silver nanoparticles, (d) β -cyclodextrin, (e) NF, (f) NFS2, (g) NFB2 and (h) NFSB.

hydrogen could reduce Ag^+ and initiate the formation of metallic silver (Ag^0).^{43,44} For this study, starch and NaOH were used as reducing agent. The antimicrobial activity of NF, NFS2, NFB2 and NFB nanofibers against *Escherichia coli* and *Staphylococcus aureus* was evaluated. Zone of inhibition under and around the nanofibrous test samples represented the antimicrobial activity.⁴⁵ Fig. 3 showed that the samples without silver nanoparticles (NF and NFB2) did not show any clear zone against the two bacteria. However, the nanofibers containing silver nanoparticles (NFS2 and NFSB) clearly exhibited inhibitory zones against the representative Gram-negative *Escherichia coli* and the representative Gram-positive *Staphylococcus aureus*. Furthermore, as interpreted from the size of clear zone, the antimicrobial activity in silver nanoparticles-loaded nanofibers was found to be more effective against *Staphylococcus aureus* than against *Escherichia coli* (Table 3). The antimicrobial difference could be due to thick bilayer lipid structure of the Gram-negative bacteria, which might limit the binding and the

Table 2 Degree of crystallinity of nanofibers

| Sample code | Degree of crystallinity (%) |
|-------------|-----------------------------|
| PVA | 35.16 |
| NF | 37.82 |
| NFS2 | 53.0 |
| NFB2 | 58.0 |
| NFSB | 60.8 |



permeability of silver nanoparticles molecules.⁴⁶ Consistent with our study, Zhang *et al.*⁴⁷ reported that the incorporation of Ag nanoparticles into PVA nanofibers could improve the antimicrobial activity of nanofibers against both Gram-positive *Staphylococcus aureus* and Gram-negative *Escherichia coli* (*E. coli*) microorganisms. They also found that the membranes show superior bacterial inhibition against Gram-positive with respect to Gram-negative bacteria.

3.4. Adsorption of volatile organic compounds

Physical adsorption of model VOC in dried solid-state nanofibrous membrane could be evaluated by noninvasive FTIR method for interactive chemical composition analysis. Fig. 4

showed FTIR spectra of rice flour, PVA, β -cyclodextrin, toluene and nanofibrous samples of NF, NFS2, NFB2 and NFSB, untreated and treated with toluene vapor. Rice flour possessed characteristic peaks at 3288 cm^{-1} (OH), 2920 cm^{-1} (C-H stretching), 1640 cm^{-1} (OH bonding of water), 1062 cm^{-1} (glycosidic linkage) and 956 cm^{-1} (C-O stretching) (Fig. 4a).^{48,49} PVA exhibited major characteristic bands at 3320 cm^{-1} (OH), 2911 cm^{-1} (C-H stretching), 1082 cm^{-1} (C-O stretching) (Fig. 4b).⁵⁰ Spectrum of β -cyclodextrin showed the characteristic peak around 3288 cm^{-1} (OH), 2920 cm^{-1} (C-H stretching) and 1015 cm^{-1} (C-O stretching) (Fig. 4c).⁵¹ While toluene exhibited characteristic bands at 3026 cm^{-1} (C-H stretching in aromatic ring), 1492 cm^{-1} (C-C stretching in aromatic ring) and 722 cm^{-1} (out of plane C-H bending) (Fig. 4d).⁵² The spectrum of NF and NFS2 nanofibers possessed characteristic peaks of rice flour and PVA, indicating that the two samples consisted of both rice flour and PVA (Fig. 4e and f). However, silver nanoparticles could not be detected by FTIR technique. With respect to NF, NFB2 and NFSB nanofibers showed new absorption peak of C-O stretching (977 cm^{-1}) (Fig. 4g and h), implying that the nanofibers composed of β -cyclodextrin. After NF, NFS2, NFB2 and NFSB nanofibers were treated with toluene, only the nanofibers with β -cyclodextrin showed new peaks at 1492 cm^{-1} (C-C stretching in aromatic ring of toluene) (Fig. 4i-l). It could be said that the nanofibers adsorbed toluene through β -cyclodextrin molecule. This result was in accordance with previous reports. Celebioglu *et al.*⁵³ prepared hydroxypropyl- β -cyclodextrin and hydroxypropyl- γ -cyclodextrin electrospun nanofibers for VOC entrapment. They found that cyclodextrin in nanofibers could entrap higher amount of VOC from their surrounding compared to their powder form due to very high surface area of the cyclodextrin-incorporated nanofibers.

3.5. Mechanical properties

From a stress-strain curve, tensile strength, modulus and elongation at break of nanofibrous membrane could be determined from the maximum stress, the slope at elastic (linear) region and the strain at break, respectively. PVA nanofibrous membrane showed tensile strength, modulus and elongation at break of 4.60 MPa, 10.44 MPa and 146.4%, respectively (Fig. 5). NF exhibited higher tensile strength (5.67 MPa) and modulus (12.45 MPa), but lower elongation at break (121.36%) than those of the PVA nanofibers. The increase of tensile strength and stiffness, as well as the reduction of extensibility of nanofibers

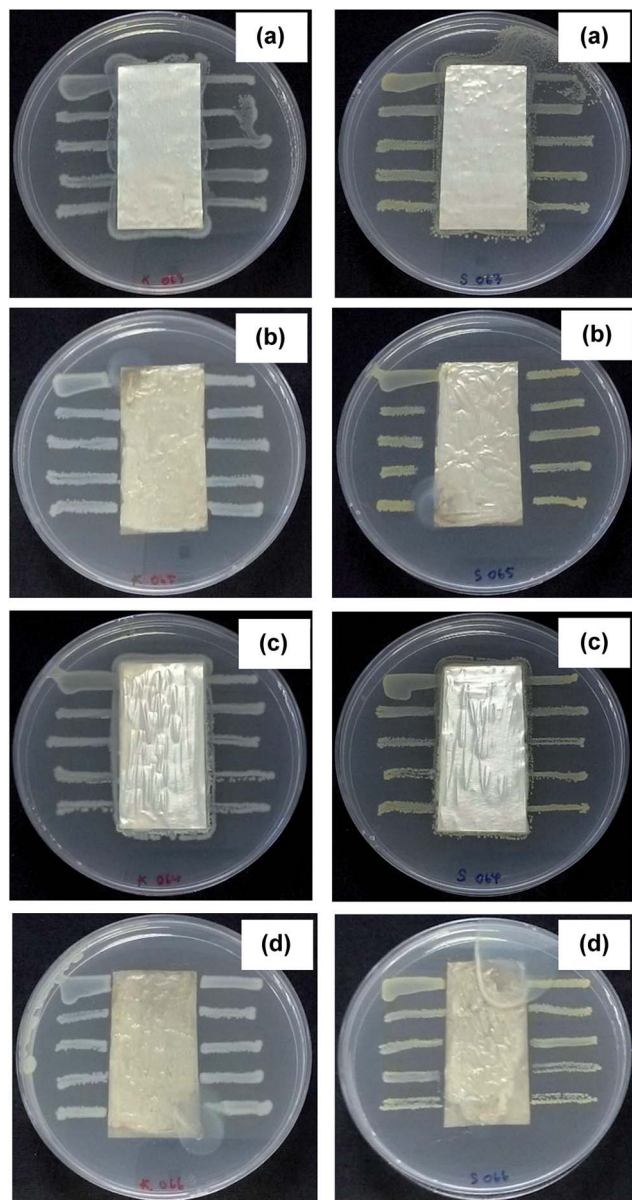


Fig. 3 Photographs taken after 24 h of incubation, showing the antibacterial activity against *Escherichia coli* (left column) and *Staphylococcus aureus* (right column) through zone of inhibition (ZOI) of different nanofibers: (a) NF, (b) NFS2, (c) NFB2 and (d) NFSB.

Table 3 Average sizes of inhibition zones for nanofibers

| Sample code | Size of inhibition zone ^a (mm) | |
|-------------|-------------------------------------------|------------------------------|
| | <i>Escherichia coli</i> | <i>Staphylococcus aureus</i> |
| NF | 0 | 0 |
| NFS2 | 0.5 ± 0.3 | 2.4 ± 0.5 |
| NFB2 | 0 | 0 |
| NFSB | 1.0 ± 0.4 | 1.6 ± 0.2 |

^a Each value represents the mean \pm SD ($n = 3$).



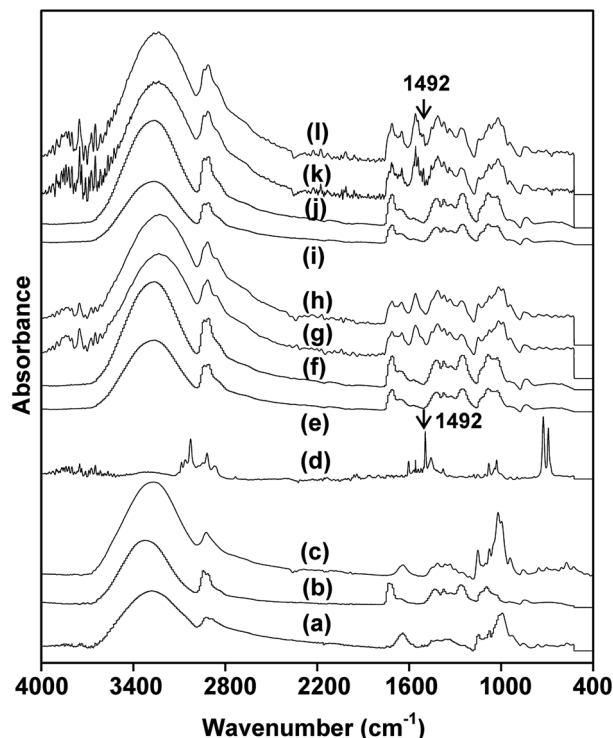


Fig. 4 FTIR spectra of (a) rice flour, (b) PVA nanofibers, (c) β -cyclodextrin, (d) toluene, (e) NF nanofibers, (f) NFS2 nanofibers, (g) NFB2 nanofibers, (h) NFSB nanofibers, (i) NF nanofibers treated with toluene vapor, (j) NFS2 nanofibers treated with toluene vapor, (k) NFB2 nanofibers treated with toluene vapor and (l) NFSB nanofibers treated with toluene vapor.

after blending with rice flour might result from the formation of intermolecular bonds between PVA and starch.³⁵ In this case, hydrogen bonding between the polymer and starch became crosslinking network which translated into the physical origin of enhanced Young's modulus. The incorporation of silver nanoparticles in NFS2, β -cyclodextrin in NFB2 or silver nanoparticles/ β -cyclodextrin in NFSB led to slightly increased tensile strength (5.69–6.15 MPa) and modulus (12.47–13.45 MPa), with decreased elongation at break (95.02–107.13%) in comparison with NF nanofibers. Previously, Sheikh *et al.* reported that the addition of silver nanoparticles to polyurethane nanofibers caused increased tensile strength.⁵⁴ Likewise, Xu *et al.* revealed that tensile strength and modulus of PVA was augmented upon addition of β -cyclodextrin, suggesting that silver nanoparticles and β -cyclodextrin act as a reinforcement for the nanofibers.⁵⁵

3.6. Air permeability of nanofibrous membranes deposited on filter paper

Air permeability represented a volume of air passing through a material per unit time per unit area. The property could be required in deciding the appropriate filter membrane for air filtration equipment. Air filter paper for general filtration exhibited air permeability of $8.63 \text{ cm}^3 \text{ s}^{-1} \text{ cm}^{-2}$. The value of air permeability with nanofibrous membrane spun for 15 minutes, 30 minutes and 60 minutes decreased in the range of 5.65–6.12

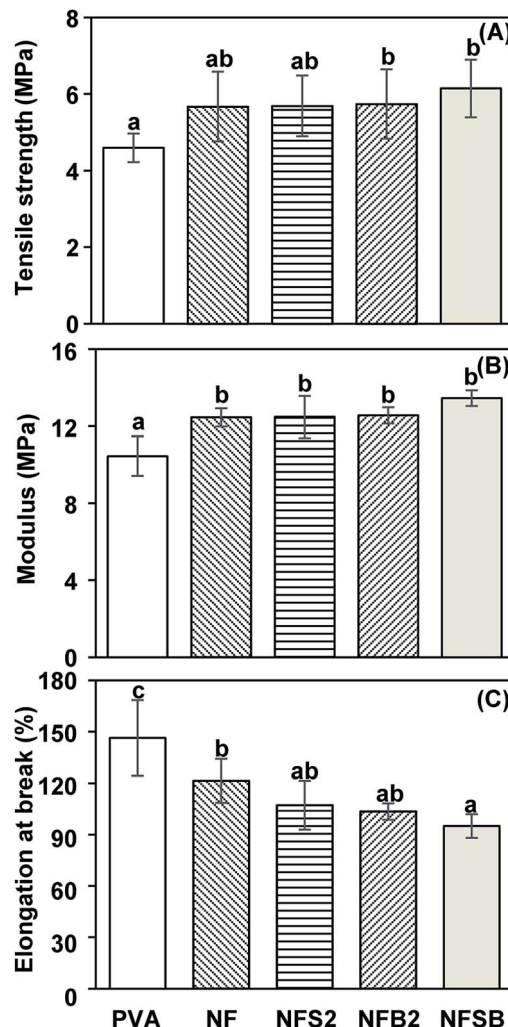


Fig. 5 (A) Tensile strength, (B) modulus and (C) elongation at break of different nanofibers. Data are reported as mean \pm SD, $n = 10$. Different small letters indicate a significant difference at $p < 0.05$ (Duncan's new multiple range test).

$\text{cm}^3 \text{ s}^{-1} \text{ cm}^{-2}$, 3.92–4.41 $\text{cm}^3 \text{ s}^{-1} \text{ cm}^{-2}$ and 0.16–0.37 $\text{cm}^3 \text{ s}^{-1} \text{ cm}^{-2}$, respectively (Table 4). The reduction of air permeability might involve the decrease of porosity in the presence of the nanofibrous membrane. In addition, air permeability of the nanofibers coated filter paper decreased with increasing

Table 4 Air permeability of nanofibers on filter paper at varying spinning time

| Sample | Air permeability ^a ($\text{cm}^3 \text{ s}^{-1} \text{ cm}^{-2}$) | | |
|--------|--------------------------------------------------------------------------------|-----------------|-----------------|
| | 15 min | 30 min | 60 min |
| PVA | 6.12 ± 0.30 | 4.41 ± 0.22 | 0.37 ± 0.06 |
| NF | 5.87 ± 0.15 | 4.23 ± 0.27 | 0.21 ± 0.04 |
| NFS2 | 6.47 ± 0.21 | 4.19 ± 0.19 | 0.22 ± 0.12 |
| NFB2 | 5.65 ± 0.29 | 3.92 ± 0.32 | 0.16 ± 0.09 |
| NFSB | 5.79 ± 0.31 | 4.08 ± 0.21 | 0.19 ± 0.11 |

^a Each value represents the mean \pm SD ($n = 3$).



spinning time. This might be due to the increased thickness of nanofibrous membrane upon spinning time. Finally, as the nanofibrous samples were evaluated against ASHRAE 52.2-2012/EN 779: 2012 standard test method, it was found that the membranes could block model dusts as small as 0.1 microns, suggesting their strong potential for multifunctional high efficiency filtration (see ESI†).

4. Conclusions

Rice flour-based biodegradable nanofibrous membranes were prepared by electrospinning technique. The contents of rice flour in solution were systematically varied an optimal condition where good processability, fibers with well-defined morphology and uniform diameter could be successfully achieved for both polymer and polymer nanocomposite. The rice flour nanofibrous membranes allowed only tiny particles (less than 0.1 micron) to pass through. Likewise, the incorporation of silver nanoparticles and β -cyclodextrin into the nanofibrous membranes led to excellent antimicrobial property and VOC-adsorption property, respectively. The results suggested the potential use of nanofibrous membranes from rice flour blends as low-environmental impact and high performance multipurpose nanofilter.

Acknowledgements

This work was financially supported by the Agricultural Research Development Agency (Public Organization), Thailand Research Organizations Network and National Research Council of Thailand.

References

- 1 S. Feng, D. Li, Z. Low, Z. Liu, Z. Zhong, Y. Hu, Y. Wang and W. Xing, *J. Membr. Sci.*, 2017, **531**, 86–93.
- 2 M. Shoeib, J. Schuster, C. Rauert, K. Su, S. Smyth and T. Harner, *Environ. Pollut.*, 2016, **218**, 595–604.
- 3 M. L. McNamara, J. Thornburg, E. O. Semmens, T. J. Ward and C. W. Noonan, *Sci. Total Environ.*, 2017, **592**, 488–494.
- 4 G. B. Hwang, K. J. Heo, J. H. Yun, J. E. Lee, H. J. Lee, C. W. Nho, G. N. Bae and J. H. Jung, *PLoS One*, 2015, **10**, 1–14.
- 5 I. Showqi, F. A. Lone, M. Ashraf, M. A. Mehmood and A. Rashid, *Nat. Env. Poll. Tech.*, 2016, **15**, 1177–1185.
- 6 S. Hou, X. Dong, J. Zhu, J. Zheng, W. Bi, S. Li and S. Zhang, *J. Colloid Interface Sci.*, 2017, **496**, 391–400.
- 7 M. Tang, J. Hu, Y. Liang and D. Y. H. Pui, *Text. Res. J.*, 2017, **87**, 498–508.
- 8 H. J. Choi, M. Kumita, S. Hayashi, H. Yuasa, M. Kamiyama, T. Seto, C. Tsai and Y. Otani, *Aerosol Air Qual. Res.*, 2017, **17**, 1052–1062.
- 9 C. Du, J. Wang, Z. Chen and D. Chen, *Appl. Surf. Sci.*, 2014, **313**, 304–310.
- 10 Y. Zhao, J. Lu, X. Liu, Y. Wang, J. Lin, N. Peng, J. Li and F. Zhao, *J. Colloid Interface Sci.*, 2016, **480**, 1–8.
- 11 X. Qin and S. Subianto, in *Electrospun Nanofibers*, ed. M. Afshari, Woodhead Publishing, Cambridge, 2017, pp. 449–466.
- 12 N. Méndez-Lozano, R. Velázquez-Castillo, E. M. Rivera-Muñoz, L. Bucio-Galindo, G. Mondragón-Galicia, A. Manzano-Ramírez and M. A. Ocampo, *Ceram. Int.*, 2017, **43**, 451–457.
- 13 F. E. Ahmed, B. S. Lalia and R. A. Hashaikeh, *Desalination*, 2015, **356**, 15–30.
- 14 G. L. Dotto, J. M. N. Santos, E. H. Tanabe, D. A. Bertuol, E. L. Foletto, E. C. Lima and F. A. Pavan, *J. Cleaner Prod.*, 2017, **144**, 120–119.
- 15 S. R. Baker, S. Banerjee, K. Bonin and M. Guthold, *Mater. Sci. Eng., C*, 2016, **59**, 203–212.
- 16 C. Salas, in *Electrospun Nanofibers*, ed. M. Afshari, Woodhead Publishing, Cambridge, 2017, pp. 73–108.
- 17 S. Thenmozhi, N. Dharmaraj, K. Kadirvelu and H. Y. Kim, *Mater. Sci. Eng. B Adv.*, 2017, **217**, 36–48.
- 18 L. Eykens, K. D. Sitter, C. Dotremont, L. Pinoy and B. V. D. Bruggen, *Sep. Purif. Technol.*, 2017, **182**, 36–51.
- 19 S. Babitha, L. Rachita, K. Karthikeyan, E. Shoba, I. Janani, B. Poornima and K. P. Sai, *Int. J. Pharm.*, 2017, **523**, 52–90.
- 20 Y. Ding, H. Hou, Y. Zhao, Z. Zhu and H. Fong, *Prog. Polym. Sci.*, 2016, **61**, 67–103.
- 21 L. Bao, K. Seki, H. Niinuma, Y. Otani, R. Balgis, T. Ogi, L. Gradon and K. Okuyama, *Sep. Purif. Technol.*, 2016, **159**, 100–107.
- 22 M. Toma and I. Fileru, *Procedia Technol.*, 2016, **22**, 969–975.
- 23 J. Wang, W. Qian, Y. He, Y. Xiong, P. Song and R. Wang, *Waste Manag.*, 2017, **65**, 11–21.
- 24 G. Liu, Z. Gu, Y. Hong, L. Cheng and C. Li, *J. Controlled Release*, 2017, **252**, 95–107.
- 25 F. Zhao, S. Chen, Q. Hu, G. Xue, Q. Ni, Q. Jiang and Y. Qiu, *Sep. Purif. Technol.*, 2017, **175**, 130–139.
- 26 A. Celebioglu, H. S. Sen, E. Durgun and T. Uyar, *Chemosphere*, 2016, **144**, 736–744.
- 27 National Nanotechnology Center, TH. Pat., 1701001837, 2017.
- 28 S. Sittipod and Y. Shi, *J. Cereal Sci.*, 2016, **69**, 398–405.
- 29 L. Amagliani, J. O'Regan, A. L. Kelly and J. A. O'Mahony, *J. Cereal Sci.*, 2016, **70**, 291–300.
- 30 S. Pancha-arnon and D. Uttapap, *Carbohydr. Polym.*, 2013, **91**, 85–91.
- 31 W. Zou, L. Yu, X. Liu, L. Chen, X. Zhang, D. Qiao and R. Zhang, *Carbohydr. Polym.*, 2012, **87**, 1583–1588.
- 32 K. Leja and G. Lewandowicz, *Pol. J. Environ. Stud.*, 2010, **19**, 255–266.
- 33 U. Shah, F. Naqash, A. Gani and F. A. Masoodi, *Compr. Rev. Food. Sci. F.*, 2016, **15**, 568–580.
- 34 S. F. Dehghan, F. Golbabaie, B. Maddah, R. Yarahmadi and A. S. Zadeh, *Int. J. Occup. Hyg.*, 2015, **7**, 110–118.
- 35 S. Woranuch, A. Pangon, K. Puagsuntia, N. Subjalearndee and V. Intasanta, *RSC Adv.*, 2017, **7**, 19960–19966.
- 36 Z. Liu and J. H. He, *Therm. Sci.*, 2014, **18**, 1473–1475.
- 37 R. Hoover, *Carbohydr. Polym.*, 2001, **45**, 253–267.
- 38 C. Yokesahachart and R. Yoksan, *Carbohydr. Polym.*, 2011, **83**, 22–31.



- 39 A. Pangon, S. Saesoo, N. Saengkrit, U. Ruktanonchai and V. Intasanta, *Carbohydr. Polym.*, 2016, **138**, 156–165.
- 40 M. Sathishkumar, K. Sneha, S. W. Won, C. W. Cho, S. Kim and Y. S. Yun, *Colloids Surf., B*, 2009, **73**, 332–338.
- 41 M. S. Zarif, A. R. Afidah, J. M. Abdullah and A. R. Shariza, *Biomed. Res.*, 2012, **23**, 513–520.
- 42 S. Prabhu and E. K. Poullose, *Int. Nano Lett.*, 2012, **2**, 1–9.
- 43 S. Iravani, H. Korbekandi, S. V. Mirmohammadi and B. Zolfaghari, *Res. Pharm. Sci.*, 2014, **9**, 385–406.
- 44 M. H. El-Rafie, H. B. Ahmed and M. K. Zahran, *Int. Sch. Res. Notices*, 2014, **702396**, 1–12.
- 45 A. R. Unnithan, N. A. M. Barakat, P. B. T. Pichiah, G. Gnanasekaran, R. Nirmala, Y. S. Cha, C. H. Jung, M. El-Newehy and H. W. Kim, *Carbohydr. Polym.*, 2012, **90**, 1786–1793.
- 46 S. N. Hazarika, K. Gupta, K. N. A. M. Shamin, P. Bhardwaj, R. Boruah, K. K. Yadav, A. Naglot, M. Mandal, R. Doley, V. Veer, I. Baruah and N. D. Namsa, *Mater. Res. Express*, 2016, **3**, 1–4.
- 47 Z. Zhang, Y. Wu, Z. Wang, X. Zou, Y. Zhao and L. Sun, *Mater. Sci. Eng., C*, 2016, **69**, 462–469.
- 48 M. Ahmad, N. M. Hani, N. P. Nirmal, F. F. Fazial, N. F. Mohtar and S. R. Romli, *Prog. Org. Coat.*, 2015, **84**, 115–127.
- 49 M. G. Lomeli-Ramírez, A. J. Barrios-Guzmán, S. García-Enriquez, J. D. J. Rivera-Prado and R. Manríquez-González, *Bioresources*, 2014, **9**, 2960–2974.
- 50 Z. Khatri, S. Ali, I. Khatri, G. Mayakrishnan, S. H. Kim and I. S. Kim, *Appl. Surf. Sci.*, 2015, **342**, 64–68.
- 51 F. D. R. Ferreira, I. B. Valentim, E. L. C. Ramones, M. T. S. Trevisan, C. Olea-Azar, F. Perez-Cruz, F. C. D. Abreu and M. O. F. Goulart, *LWT-Food Sci. Technol.*, 2013, **51**, 129–134.
- 52 X. Li, Z. Zhu, Q. Zhao and S. Liu, *Appl. Surf. Sci.*, 2011, **257**, 4709–4714.
- 53 A. Celebioglu, H. S. Sen, E. Durgun and T. Uyar, *Chemosphere*, 2014, **144**, 736–744.
- 54 F. A. Sheikh, N. A. M. Barakat, M. A. Kanjwal, S. H. Jeon, H. S. Kang and H. Y. Kim, *J. Appl. Polym. Sci.*, 2010, **115**, 3189–3198.
- 55 J. Xu, X. Li, F. Sun and P. Cao, *J. Biomat. Sci. Polym. E.*, 2010, **21**, 1023–1038.

